RESILIENT RESPONSE OF GRANULAR MATERIALS SUBJECTED TO TIME-DEPENDENT LATERAL STRESSES

John J. Allen, Department of Civil Engineering,
United States Air Force Academy; and
Marshall R. Thompson, Department of Civil Engineering,
University of Illinois at Urbana-Champaign

Present methods of determining the resilient parameters (modulus of deformation and Poisson's ratio) of granular materials for use in the analysis of pavement structures subjected to moving wheel loads are based on the results of laboratory repeated-load triaxial tests in which the minor principal stress (chamber pressure) is held constant. However, as a wheel load moves over an element of an actual pavement structure, the element is subjected to both time-dependent lateral and vertical stresses. The purpose of this study was to determine the effects of this nonconstant state of stress on the observed resilient properties of granular materials. Based on the current literature, certain factors thought to affect the resilient properties of granular materials were identified. Among these factors, which were later investigated during the laboratory phase, were density level, type of material, load duration, and number of load repetitions. Nonlinear, finite-element analyses of typical pavement sections were used to establish typical horizontal and vertical stress pulses. The characteristic stress pulses were used to test specimens during the laboratory investigation. It was shown that factors such as load duration, stress sequence, and number of repetitions have negligible effects on the resilient parameters. Nonlinear regression analyses of the laboratory data indicated that the resilient modulus is significantly influenced by the state of stress in the material and may be expressed as a function of the first invariant of the stress tensor. Poisson's ratio may be expressed as a function of the principal stress ratio. The effects of density and material type are small compared with the stress-dependent effects. The resilient modulus determined by the constant-confining-pressure test was found to vary insignificantly from that determined by the variable-confining-pressure test. However, the constant-confining-pressure test data greatly overestimate Poisson's ratio because of the anisotropic nature of the material and the greater volume change that is observed in that type of test.

•ACCURATE prediction of the fatigue life of flexible pavements depends on proper assessment of stress and strain in the pavement under moving loads. Accuracy in pavement structural analysis has been facilitated by finite-element analytical techniques and layered, elastic computer solutions. But, paving materials must be characterized for use with these computer techniques. Therefore, efforts have been made to determine essential stress-strain relations for pavement components.

OBJECT

The object of this research was to assess the effects of nonconstant lateral pressures on the resilient response of granular materials. Predictive equations for material

Publication of this paper sponsored by Committee on Strength and Deformation Characteristics of Pavement Sections.

stiffness and Poisson's ratios were developed and are considered accurate for use in various analytical techniques, insofar as they are applied to the proper boundary value problem. That is, these are pseudoelastic material parameters that define the response of an unbound granular base-course material to stresses applied at typical vehicle speeds. These results are not intended to serve as a model for predicting accumulated plastic deformations (rutting). But, they have direct application to the problem of predicting transient, "resilient" pavement deflections, and, therefore, serve as a step toward the successful prediction of flexible pavement fatigue life.

Despite the knowledge of the heavy influence of confining stresses on the resilient parameters, there have been no published results of tests where lateral stresses were varied simultaneously with axial stress on a time scale that would simulate transient wheel loadings. Because this condition represents the stress that occurs in an actual pavement structure subjected to moving wheel loads, the purpose of this research was to simulate field conditions in the laboratory by repeated-load, variable-confining-pressure, triaxial tests.

STRESS PULSES IN FLEXIBLE PAVEMENT SYSTEMS

Three pavement structural sections were analyzed by a nonlinear finite-element technique:

1. A runway section consisting of 3 in. (7.6 cm) of asphalt concrete, 6 in. (15.2 cm) of granular base, 15 in. (38.1 cm) of granular subbase over a subgrade with a CBR equal to 4;
2. A highway section consisting of 3 in. (7.6 cm) of asphalt concrete, 6 in. (15.2 cm) of granular base, 10 in. (25.4 cm) of granular subbase over a subgrade with a CBR equal to 4; and
3. An "inverted" section similar to the highway section except that the granular subbase was replaced by a 10-in.- (25.4-cm-) thick lime-stabilized subgrade layer.

A uniform surface pressure of 100 psi (690 kPa) distributed over a circular area with a 10-in. (25.4-cm) radius was applied to the runway section. For the other 2 sections the surface pressure was 80 psi (552 kPa) and the radius was 6 in. (15.2 cm). All material properties were chosen as representative values that were determined from a literature survey.

For all 3 sections, the shapes of the stress distributions were related to their depth within the section. The major principal stress pulse and the vertical stress pulse, although generally sinusoidal, were peaked more sharply in the upper part of the base course and had shallower slopes in the lower base and subbase. Major principal stresses are always greater than vertical stresses, except directly under the center of the load where they are equal. Therefore, the major principal stress pulse was somewhat longer than the vertical stress pulse. This difference increased with depth. Barksdale reported the same trends (2).

Radial and minor principal stress pulses were similar in shape for the runway and highway sections. These pulse shapes also were related to depth within the system. In the upper portions of the base, these pulses were more or less flat-topped. In the extreme upper portion of the base the stresses were not exactly under the center of the load, but at a slight radial offset. Both types became more sinusoidal as depth increased.

Analysis of the inverted section revealed significant changes in stress distributions. Although the vertical and major principal stress pulses were the same shape as those for the highway section, their magnitudes were as much as 100 percent greater throughout the granular layer. More significant, though, was the drastic increase in the radial and minor principal stresses throughout the granular layer of the inverted section. The reduction in confining pressure beneath the center of the load was eliminated completely and a sinusoidal pulse shape resulted. The magnitude of the minor principal stress pulse directly under the load increased by 500 to 800 percent. As discussed by Allen, the increased stress levels in the granular layers of the inverted section exert significant influence over the load response of the pavement structure (1). The use of a buried

stabilized layer is 1 method of exploiting the stress-dependent nature of granular paving materials to the designer's advantage.

The half-sinusoid was selected as the basic pulse shape for this study because it is the most general shape of all stress distributions and because most standard laboratory function generators, in combination with hydraulic testing equipment, can apply it. Simulation of stress at various depths within the granular layer was accomplished by varying the pulse duration and magnitude.

LABORATORY TESTING PROGRAM

Materials

The following materials were tested during this study:

1. A well-graded crushed limestone,
2. A well-graded siliceous gravel, and
3. A blend of the gravel and limestone.

The blend was obtained by adding equal percentages of the crushed stone and gravel on the No. 4 sieve to the gravel material passing the No. 4. The maximum size of the aggregate was 1½ in. (3.81 cm) with 5 percent passing the No. 200 sieve. The plasticity index was 5 for the crushed stone and 9 for the gravel. All specimens were prepared to the same gradation.

Specimen Preparation

All specimens were prepared on the chamber base plate by drop-hammer compaction in a 6- by 12-in. (15.2- by 30.5-cm) split mold that attached to the base plate by tie rods and wing nuts. The hammer had a 2.0-in. (5.1-cm) diameter striking face, weighed 10 pounds (4.5 kg), and had a fall of 18 in. (45.7 cm). Specified densities were attained by varying the number of layers per specimen and the number of blows per layer.

Each specimen was encased in 2 latex membranes to prevent leakage during the test. This procedure was effective because when moisture contents were determined after testing, they varied only minimally from the original moisture contents.

Nine specimens were tested during the primary test series (3 materials and 3 density levels). Table 1 gives the properties of the specimens. The high density and accompanying moisture content given in Table 1 corresponded to maximum density and optimum moisture resulting from an AASHO T 180 compaction. The low density and optimum moisture content corresponded to the maximum density and optimum moisture from the AASHO T 99 test. The intermediate levels were moisture-density values between the peaks of the 2 compaction curves.

Because the object of this study was to compare the response of the specimens to the 2 types of stress pulses (variable and constant confining pressures), and because these were nondestructive tests, only 1 specimen of each material at any density level was tested. The preliminary test series indicated that any 1 specimen could be tested at all stress levels without significantly affecting the results. This procedure eliminated the possibility that unplanned specimen-to-specimen variations in density and moisture content would occur.

Testing Equipment and Instrumentation

The laboratory investigation portion of this study was conducted at the U.S. Army Corps of Engineers Construction Engineering Research Laboratory at Champaign, Illinois. The unique aspect of this study, that is, the requirement that the triaxial chamber confining pressure be varied simultaneously with the axial load, was satisfied by a closed-loop testing system. Axial stress was applied to the specimen through a hydraulic-actuated piston. The chamber pressure was varied by a hydraulic-actuated piston that reacted directly on the chamber fluid; water, in this case. Program input was provided by 2 function generators, 1 connected to the axial load controller and the other connected to the confining pressure controller. It was necessary to use 2 function generators to allow for a slight delay in the confining pressure pulse. This delay was

caused by compressibility of the chamber fluid and friction loss in the line connecting the chamber and the chamber pressure supply. This procedure made it possible to apply lateral and axial stress pulses to the specimen simultaneously.

The axial load was monitored by a load cell mounted on the test frame above the triaxial chamber. Chamber pressure was monitored by a pressure transducer installed at the base of the triaxial chamber. Axial deformation was measured over the central half of the specimen by 2 optical trackers.

Radial deformation was measured by sensors [4-in.- (10.2-cm-) diameter, disk-shaped coils of wire] that were mounted at midheight of the specimen and held in place by a 2-in.- (5.1-cm-) wide rubber strip cut from a triaxial membrane.

A dial gauge mounted on top of the triaxial chamber and a linear variable differential transformer on the actuator of the test frame were used to monitor nonrecoverable deformations and provided a backup system for obtaining resilient strain data. All stress and deformation data were recorded on an 8-track oscillograph printer.

Preliminary Tests

To aid in designing the primary test series, the following 3 preliminary tests, described in detail by Allen (1), were carried out on the crushed stone and gravel specimens:

1. A stress history test in which the specimens were subjected to 10,000 stress repetitions at 2 stress levels;
2. A stress sequence test in which the specimens were subjected to 100 stress repetitions at each of several increasing and decreasing stress levels; and
3. A stress pulse duration test in which the pulse duration was varied from 0.04 to 1.00 second.

These tests on both material types yielded results similar to those reported by Hicks (8). Specifically, the resilient response of these materials after 25 to 100 stress repetitions represented the response determined after several thousand stress repetitions; 1 specimen could be used to measure the resilient response over a wide range of stress levels, and these stresses could be applied in any order; and, the resilient response of these materials was affected only minimally by variations from 0.04 to 1.00 second in stress pulse duration.

Based on the preliminary test results, the stress levels given in Table 2 were selected for the primary test series. They were applied to each specimen in the order given and had a pulse duration of 0.15 sec and a frequency of 20 repetitions per min.

PRIMARY TEST SERIES

Methods of Computing Resilient Modulus, E_r, and Resilient Poisson's Ratio, ν_r

The resilient modulus, as computed from results of constant-confining-pressure triaxial tests (CCP tests), is the ratio of the repeated deviator stress, σ_1-σ_3, to recoverable axial strain, ϵ_a. The resilient Poisson's ratio is the ratio of recoverable lateral strain, ϵ_l, to recoverable axial strain, ϵ_a. This method of computation is the same as would apply to an isotropic, linear, elastic material under uniaxial stress conditions. The nature of the CCP test, in which the specimen consolidates under a constant chamber pressure before the dynamic increment of stress is applied in the axial direction, has led to general acceptance of this method of determining resilient parameters. However, the nature of the variable-confining-pressure triaxial test (VCP test), in which lateral stress is applied dynamically and simultaneously with axial stress, is such that to compute the resilient modulus as described above would ignore the effect of Poisson's ratio on axial strains and overestimate the modulus. Therefore, it was necessary to use the 3-dimensional stress-strain relations for isotropic, linear, elastic material:

Table 1. Test specimens.

Specimen	Material	Density (lb/ft^3)	Moisture (percent)	Saturation (percent)
HD-1	Crushed stone	138.0, high	5.7	78
MD-1	Crushed stone	134.0, intermediate	6.3	73
LD-1	Crushed stone	130.0, low	7.0	70
HD-2	Gravel	139.4, high	6.3	82
MD-2	Gravel	134.0, intermediate	6.5	74
LD-2	Gravel	131.0, low	6.7	69
HD-3	Blend	139.5, high	6.3	88
MD-3	Blend	134.5, intermediate	6.8	78
LD-3	Blend	131.0, low	7.2	74

Note: 1 lb/ft^3 = 16 kg/m^3.

Table 2. Test schedule.

Stress Level (psi)			Confining Pressure	Stress Level (psi)			Confining Pressure
σ_3	σ_1	σ_1/σ_3		σ_3	σ_1	σ_1/σ_3	
2	8	4	Variable	8	56	7	Variable
2	12	6	Variable	8	12	1.5	Constant
2	16	8	Variable	8	24	3	Constant
2	8	4	Constant	8	40	5	Constant
2	12	6	Constant	8	56	7	Constant
2	16	8	Constant	11	22	2	Constant
5	10	2	Constant	11	44	4	Constant
5	15	3	Constant	11	66	6	Constant
5	25	5	Constant	11	22	2	Variable
5	35	7	Constant	11	44	4	Variable
5	45	9	Constant	11	66	6	Variable
5	10	2	Variable	15	25	1.6	Variable
5	15	3	Variable	15	45	3	Variable
5	25	5	Variable	15	60	4	Variable
5	35	7	Variable	15	75	5	Variable
5	45	9	Variable	15	25	1.6	Constant
8	12	1.5	Variable	15	45	3	Constant
8	24	3	Variable	15	60	4	Constant
8	40	5	Variable	15	70	4.7	Constant

Note: All stress levels were applied for 100 repetitions. One pulse duration of 0.15 second was used.
1 psi = 6.89 kPa.

Table 3. Regression equations for E_r models from primary test data.

Specimen	Type of Test	Model, $E_r = f(\theta)$			Model, $E_r = f(\sigma_3)$		
		Equation	Correlation Coefficient	Standard Error	Equation	Correlation Coefficient	Standard Error
HD-1	VCP	$6,635\theta^{0.40}$	0.930[a]	3,144	$18,010\sigma_3^{0.28}$	0.669[b]	6,338
MD-1	VCP	$1,793\theta^{0.70}$	0.992[a]	1,463	$8,556\sigma_3^{0.57}$	0.794[a]	7,014
LD-1	VCP	$2,113\theta^{0.65}$	0.982[a]	2,058	$8,410\sigma_3^{0.57}$	0.819[a]	6,227
HD-2	VCP	$7,766\theta^{0.32}$	0.767[a]	3,996	$18,480\sigma_3^{0.19}$	0.515[c]	5,338
MD-2	VCP	$6,995\theta^{0.33}$	0.906[a]	2,202	$15,738\sigma_3^{0.23}$	0.664[b]	3,897
LD-2	VCP	$1,613\theta^{0.69}$	0.973[a]	2,033	$7,924\sigma_3^{0.51}$	0.781[a]	5,473
HD-3	VCP	$6,891\theta^{0.45}$	0.980[a]	2,035	$18,951\sigma_3^{0.35}$	0.832[a]	5,638
MD-3	VCP	$7,725\theta^{0.33}$	0.981[a]	1,042	$15,806\sigma_3^{0.26}$	0.841[a]	2,890
LD-3	VCP	$4,562\theta^{0.43}$	0.856[a]	3,367	$14,516\sigma_3^{0.24}$	0.498[c]	5,648
HD-1	CCP	$2,376\theta^{0.68}$	0.997[a]	1,149	$12,454\sigma_3^{0.55}$	0.845[a]	7,896
MD-1	CCP	$4,928\theta^{0.46}$	0.973[a]	1,950	$14,254\sigma_3^{0.39}$	0.872[a]	4,115
LD-1	CCP	$3,083\theta^{0.59}$	0.962[a]	3,132	$11,068\sigma_3^{0.53}$	0.909[a]	4,813
HD-2	CCP	$4,596\theta^{0.50}$	0.741[a]	8,063	$11,128\sigma_3^{0.54}$	0.803[a]	7,157
MD-2	CCP	$8,016\theta^{0.31}$	0.803[a]	3,551	$14,729\sigma_3^{0.31}$	0.838[a]	3,247
LD-2	CCP	$2,849\theta^{0.56}$	0.882[a]	4,289	$8,517\sigma_3^{0.55}$	0.916[a]	3,641
HD-3	CCP	$5,989\theta^{0.48}$	0.932[a]	4,254	$16,433\sigma_3^{0.45}$	0.922[a]	4,542
MD-3	CCP	$6,459\theta^{0.37}$	0.829[a]	3,977	$13,379\sigma_3^{0.37}$	0.873[a]	3,471
LD-3	CCP	$2,966\theta^{0.60}$	0.882[a]	4,962	$9,079\sigma_3^{0.58}$	0.914[a]	4,260

[a]Significant at $\alpha = 0.001$. [b]Significant at $\alpha = 0.01$. [c]Significant at $\alpha = 0.05$.

Table 4. Regression equations for υ_r models from primary test data.

Specimen	Type of Test	$\upsilon_r = f(\sigma_1/\sigma_3)$	Correlation Coefficient	Standard Error
HD-1	VCP	$0.62 - 0.19 (\sigma_1/\sigma_3) + 0.04 (\sigma_1/\sigma_3)^2 - 0.002 (\sigma_1/\sigma_3)^3$	0.907[a]	0.026
MD-1	VCP	$0.47 - 0.07 (\sigma_1/\sigma_3) + 0.02 (\sigma_1/\sigma_3)^2 - 0.001 (\sigma_1/\sigma_3)^3$	0.838[a]	0.045
LD-1	VCP	$0.60 - 0.14 (\sigma_1/\sigma_3) + 0.02 (\sigma_1/\sigma_3)^2 - 0.0007 (\sigma_1/\sigma_3)^3$	0.881[a]	0.036
HD-2	VCP	$-0.12 + 0.45 (\sigma_1/\sigma_3) - 0.09 (\sigma_1/\sigma_3)^2 + 0.005 (\sigma_1/\sigma_3)^3$	0.645[b]	0.085
MD-2	VCP	$0.46 + 0.01 (\sigma_1/\sigma_3) - 0.01 (\sigma_1/\sigma_3)^2 + 0.002 (\sigma_1/\sigma_3)^3$	0.889[a]	0.026
LD-2	VCP	$0.70 - 0.22 (\sigma_1/\sigma_3) + 0.04 (\sigma_1/\sigma_3)^2 - 0.002 (\sigma_1/\sigma_3)^3$	0.925[a]	0.027
HD-3	VCP	$0.49 + 0.01 (\sigma_1/\sigma_3) - 0.01 (\sigma_1/\sigma_3)^2 + 0.001 (\sigma_1/\sigma_3)^3$	0.766[a]	0.037
MD-3	VCP	$0.50 - 0.02 (\sigma_1/\sigma_3) - 0.003 (\sigma_1/\sigma_3)^2 + 0.0006 (\sigma_1/\sigma_3)^3$	0.561[c]	0.048
LD-3	VCP	$0.52 - 0.07 (\sigma_1/\sigma_3) + 0.006 (\sigma_1/\sigma_3)^2 + 0.0002 (\sigma_1/\sigma_3)^3$	0.840[a]	0.026
HD-1	CCP	$-0.17 + 0.30 (\sigma_1/\sigma_3) - 0.04 (\sigma_1/\sigma_3)^2 + 0.002 (\sigma_1/\sigma_3)^3$	0.895[a]	0.047
MD-1	CCP	$0.29 + 0.12 (\sigma_1/\sigma_3) - 0.01 (\sigma_1/\sigma_3)^2 + 0.0006 (\sigma_1/\sigma_3)^3$	0.746[a]	0.060
LD-1	CCP	$-0.01 + 0.28 (\sigma_1/\sigma_3) - 0.04 (\sigma_1/\sigma_3)^2 + 0.002 (\sigma_1/\sigma_3)^3$	0.723[a]	0.096
HD-2	CCP	$-0.14 + 0.46 (\sigma_1/\sigma_3) - 0.06 (\sigma_1/\sigma_3)^2 + 0.003 (\sigma_1/\sigma_3)^3$	0.429[d]	0.208
MD-2	CCP	$0.95 - 0.22 (\sigma_1/\sigma_3) + 0.04 (\sigma_1/\sigma_3)^2 - 0.002 (\sigma_1/\sigma_3)^3$	0.654[b]	0.144
LD-2	CCP	$-0.04 + 0.32 (\sigma_1/\sigma_3) - 0.05 (\sigma_1/\sigma_3)^2 + 0.003 (\sigma_1/\sigma_3)^3$	0.953[a]	0.056
HD-3	CCP	$-0.16 + 0.37 (\sigma_1/\sigma_3) - 0.05 (\sigma_1/\sigma_3)^2 + 0.003 (\sigma_1/\sigma_3)^3$	0.868[a]	0.073
MD-3	CCP	$-0.02 + 0.27 (\sigma_1/\sigma_3) - 0.03 (\sigma_1/\sigma_3)^2 + 0.001 (\sigma_1/\sigma_3)^3$	0.828[a]	0.091
LD-3	CCP	$-0.09 + 0.36 (\sigma_1/\sigma_3) - 0.05 (\sigma_1/\sigma_3)^2 + 0.003 (\sigma_1/\sigma_3)^3$	0.729[a]	0.121

[a]Significant at $\alpha = 0.001$. [b]Significant at $\alpha = 0.01$. [c]Significant at $\alpha = 0.02$. [d]Significant at $\alpha = 0.1$.

Figure 1. VCP test results—$E_r = f(\theta)$ model, specimen MD-1.

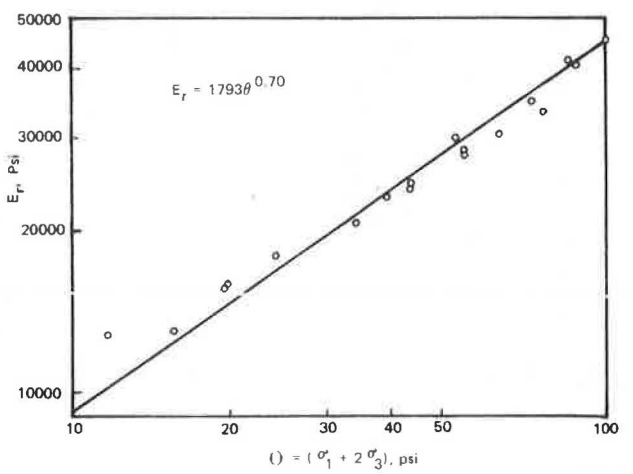

Figure 2. VCP test results—$\upsilon_r = f(\sigma_1/\sigma_3)$ model, specimen LD-2.

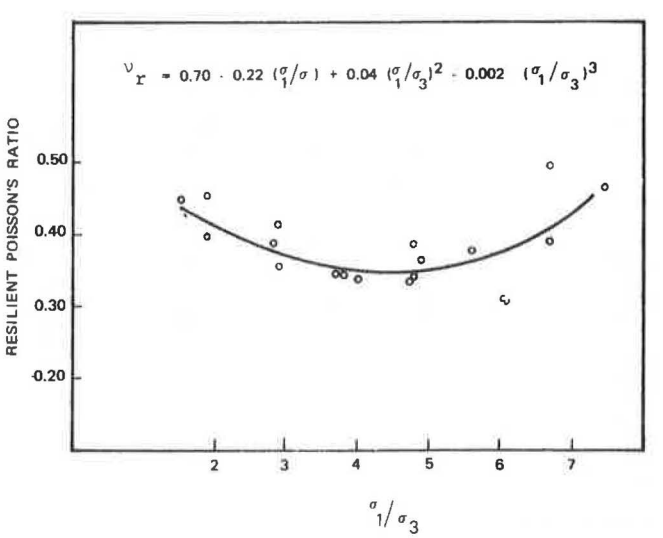

$$\epsilon_a = \frac{1}{E_r}(\sigma_a - 2\nu_r\sigma_r)$$
$$\epsilon_\ell = \frac{1}{E_r}[\sigma_a - \nu_r(\sigma_a + \sigma_r)] \quad (1)$$

where

σ_a = axial stress,
σ_r = radial stress,
ϵ_a = recoverable axial strain,
ϵ_ℓ = recoverable lateral (radial) strain,
E_r = resilient modulus, and
ν_r = resilient Poisson's ratio.

Statistical Analysis of Data

The VCP and CCP test data were analyzed by using linear regression techniques. E_r and ν_r were correlated with stress parameters σ_3; σ_1/σ_3; $\sigma_1 - \sigma_3$; and θ, the sum of the principal stresses. Comparison of the correlation coefficients and standard errors of the various models made possible selections of the models that most accurately fit the laboratory data. The data were analyzed by nonlinear regression techniques and the following models resulted:

$$E_r = K\,\theta^n$$
$$E_r = K'\sigma_3^{n'}$$
$$\nu_r = b_0 + b_1(\sigma_1/\sigma_3) + b_2(\sigma_1/\sigma_3)^2 + b_3(\sigma_1/\sigma_3)^3 \quad (2)$$

where

K, n, K′, n′, and b = constants from regression analysis;
$\theta = \sigma_1 + 2\sigma_3$;
σ_3 = minor principal stress; and
σ_1 = major principal stress.

The model for E_r based on θ yielded the highest correlation coefficients and lowest standard errors of all the models. But, the considerable scatter in the data associated with the σ_3 model resulted because it did not account for the effects of the axial stress on E_r. It is included because it has been proposed by other investigators. Tables 3 and 4 give the results of the statistical analyses.

Effects of Stress

Primary test results demonstrated that the resilient material parameters were affected much more significantly by changes in stress than by changes in any other factors. For example, the resilient modulus changed by as much as 400 percent over the range of stress encountered in a typical pavement system. The VCP and CCP test data show variations in the resilient modulus computed for different values of σ_1 at any 1 value of σ_3.

The model relating E_r to the first invariant of the stress tensor, θ, reduced the scatter in the data by accounting for the effects of all 3 principal stresses. Figure 1 shows this relation for intermediate density crushed stone, specimen MD-1. The higher correlation coefficients and lower standard errors associated with the θ model as compared to the σ_3 model also were obtained for the other specimens. The increase in E_r as θ increased is evident; Figure 1 indicates a 400 percent increase in E_r as θ increased from 10 to 80 psi (69 to 552 kPa). Although data from only 1 specimen are presented in Figure 1, the same trends were evident from the results obtained for all specimens.

The stress-dependent nature of the resilient Poisson's ratio is shown in Figure 2. The best fit to the laboratory data was obtained for all specimens by expressing ν_r as a function of σ_1/σ_3 (Eq. 2). Figure 2 shows this relationship for the VCP test data from

low density gravel, specimen LD-2. Of interest is the relatively flat slope of the curve through the range 2 to 7. This indicates that, because this range of stress ratios is typical of that found in pavement systems, pavement analyses that are based on a representative constant value of Poisson's ratio for granular layers might be appropriate. The validity of this observation is strengthened by the fact that the VCP test results for all specimens yielded for the same range of σ_1/σ_3 Poisson's ratio values very close to those shown in Figure 2.

Figure 3 shows ν_r values from the CCP test on the same specimen as shown in Figure 2. This figure, typical of the CCP results for all specimens, differs in 2 respects from the typical VCP results shown in Figure 2. First, the curve is concave downward throughout the range of interest, whereas the curve in Figure 2 is concave upward. Second, the values of ν_r are much higher (> 0.50) throughout the same range of σ_1/σ_3 for the CCP results than for the VCP. This contrast may indicate that the CCP test conditions caused the specimen to undergo more volume change than did the VCP test.

Effects of Density

The effects of variations in dry density, γ_d, on E_r are shown in Figure 4. In general, density effects were more pronounced at lower values of θ than at higher values. As Figure 4 indicates, there was a general trend of increasing E_r values as γ_d increased. The convergent regression lines in Figure 4 reveal that, at large values of θ, lower density specimens may exhibit stiffer load response than higher density specimens.

The VCP test data showed very slight differences in ν_r values for various density levels. High density specimens had lower values of ν_r than did the lower density specimens, although there were exceptions. For the gravel and blend specimens, the low density specimens showed lower ν_r values except at the upper extreme of σ_1/σ_3 values. No trends were evident from the CCP data, except that ν_r, obtained from the CCP test, was always greater than that obtained from the VCP test data. Again, this would seem to indicate that greater volume changes are caused by the CCP test conditions.

Effects of Type of Material

Figure 5 shows the effects of type of material on the resilient modulus. The intersecting regression lines indicate that the differences in the moduli for different materials were functions of stress. For all specimens the crushed stone generally yielded greater values for the resilient modulus than did the gravel throughout the entire range of θ values.

The VCP test results indicate almost identical values of ν_r for all 3 materials at the lowest density level. There is not much difference between the regression lines for the other density level specimens, but gravel displayed consistently higher values of Poisson's ratio than did crushed stone or blend material. Again, the relatively flat nature of the regression curves from 2 to 7 was noted.

The CCP test data show considerably more variation in ν_r values for different material types, but no firm conclusions can be reached. Crushed stone displayed the lowest values of ν_r for the high and low density specimens, but gravel yielded the highest values for the high density specimens, the intermediate values of ν_r for the low density specimens, and the lowest Poisson's ratio for the intermediate density specimens. Here, too, the CCP test results yielded consistently higher values of Poisson's ratio than did the VCP results.

Plastic Deformations

Although no direct attempts were made to measure the plastic (nonrecoverable) deformations associated with the individual stress pulses, data are available that show total plastic deformations accumulated by each specimen throughout the test series (1). These data indicate that nonrecoverable deformations associated with the CCP test exceeded those associated with the VCP test for every specimen.

Figure 3. CCP test results—$\upsilon_r = f(\sigma_1/\sigma_3)$ model, specimen LD-2.

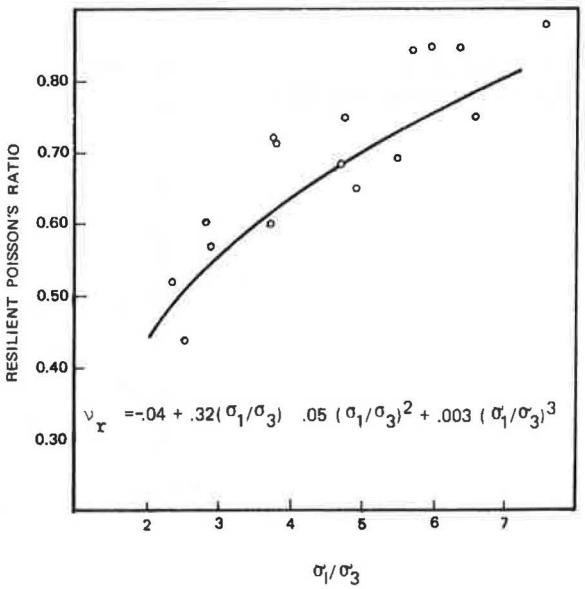

Figure 4. VCP test results—$E_r = f(\theta)$ model, specimens HD-2, MD-2, and LD-2.

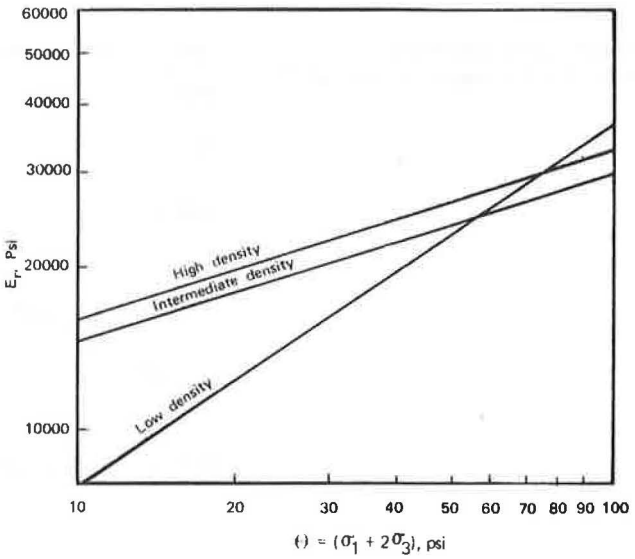

Figure 5. VCP test results—$E_r = f(\theta)$ model, specimens LD-1, LD-2, and LD-3.

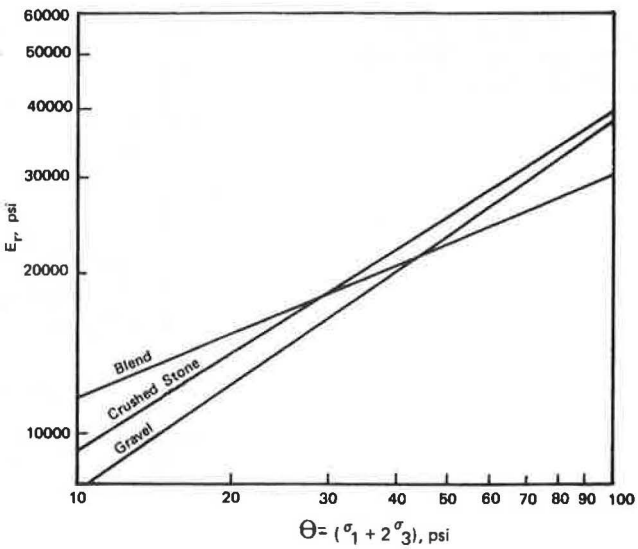

Figure 6. VCP and CCP test results—$E_r = f(\theta)$ model, specimen MD-1.

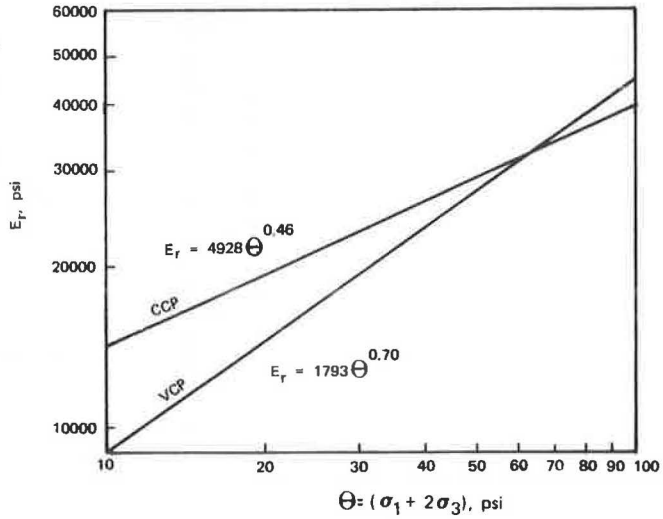

Figure 7. VCP and CCP test results—$E_r = f(\theta)$ model, specimen HD-2.

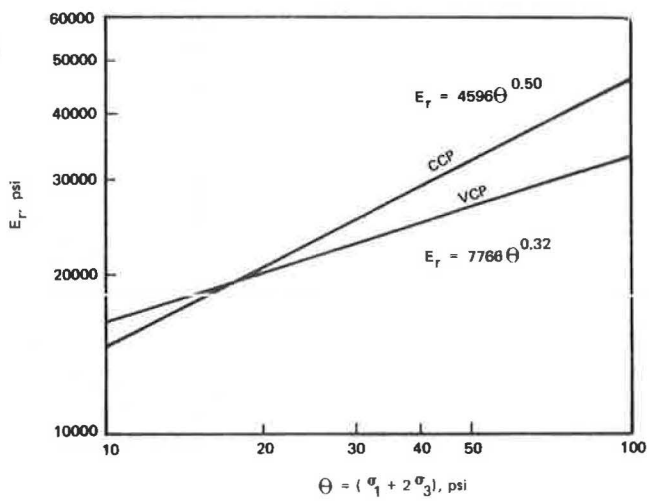

Figure 8. Comparison of VCP and CCP test results—$E_r = f(\theta)$ model, specimens HD-3 and MD-3.

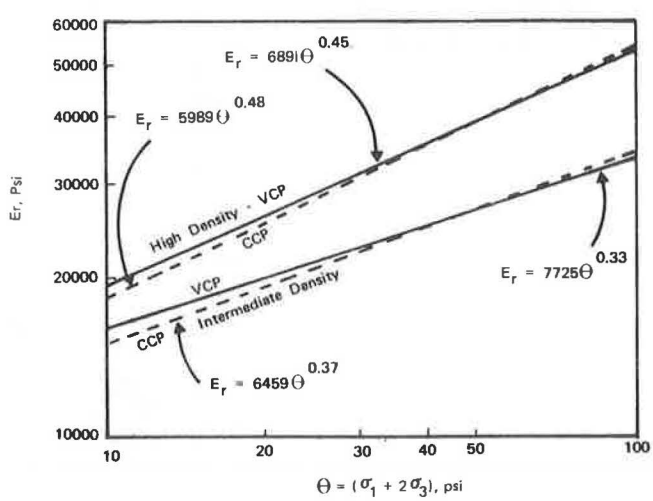

Anisotropic Behavior

Elastic isotropic materials cannot have a Poisson's ratio value in excess of 0.5. However, as was reported earlier, the CCP test results yielded values of ν_r consistently in excess of 0.5. Certainly, a percentage of the large lateral deformations involved are due to the nonuniform stress and strain states within the specimens; but, it can also be assumed that these results indicate anisotropic behavior by granular materials. The same conclusion has been reached by Moore, Britton, and Scrivner (9); Barksdale and Hicks (4); and Dehlen (5).

At principal stress ratios, σ_1/σ_3, in the range from 2 to 7, which is typical of those thought to exist in granular layers of flexible pavement systems, this anisotropic behavior was not observed in the VCP test series, as evidenced by the consistently lower Poisson's ratio values. However, at stress ratios approaching hydrostatic conditions, the measured lateral deformations were so large as to be incompatible with isotropic material properties. This indicates that the stiffness of the material was less in the lateral direction than in the axial direction. Dehlen (5) reported similar cross-isotropic behavior of sands. Despite the evidence of some degree of anisotropic properties of the materials tested, the VCP test data indicate that, in the proper range of stress states, such behavior only minimally influences the results.

Comparison of VCP and CCP Test Results

Test results for the crushed stone and gravel materials indicate that the CCP test yielded slightly higher values of E_r throughout the range of θ values for the intermediate and low density specimens than did the VCP test. This was also true for the low density blend specimen for values of θ greater than 15 psi (103 kPa). The difference in E_r values in each case was maximum for values of θ near 10 psi (69 kPa), the lower extreme for θ. At this point, the CCP test on the intermediate density crushed stone specimen showed E_r to be approximately 50 percent greater than the VCP test data indicated. This difference diminished as θ increased because the regression lines converged at higher θ values. However, the differences in E_r for the other specimens were considerably smaller, 30 percent at maximum. Figures 6 and 7 show the variation in E_r for the CCP and VCP test data derived from specimens MD-1 and HD-2.

Similar results were obtained from the high density crushed stone and gravel specimens. For gravel, the CCP and VCP test regression lines intersected at a θ value near 17 psi (117 kPa); so for most of the range of interest the CCP test results yielded higher values of E_r. But for the crushed stone specimen, the point of intersection was at a θ value of 35 psi (241 kPa).

For 2 specimens, the high and intermediate density blend specimens, the VCP and CCP test data resulted in almost identical regression lines for E_r, as shown in Figure 8.

It would appear that, in general, the CCP test data overestimated the resilient modulus as compared to the VCP test data. However, 2 observations should be made. First, this phenomenon was not observed for all specimens. Second, in the cases where it did occur, the magnitude of the difference in E_r was not constant because of the intersecting or convergent nature of the regression lines; therefore, the magnitude of the difference depends on the value of θ for which the values of E_r are calculated. The differences in the results of the 2 types of test may or may not be significant for pavement response to load because the modulus throughout the granular layers was determined from existing stress. The significance of these differences in predictive equations for E_r is discussed by Allen (1).

The CCP test data for all specimens yielded significantly higher values for the resilient Poisson's ratio than did the VCP data, which indicates correspondingly greater volume change. It can be shown that the volumetric strain of a specimen, $\Delta v/v$, is equal to the first invariant of the strain tensor, $\epsilon_1 + 2\epsilon_3$, for the triaxial test specimen. Detailed test data (not included in this paper) showed that at almost all stress levels applied during the CCP test, the $\Delta v/v$ calculated from the sum of the principal strains would indicate that the specimen increased in volume. However, applying the same procedure to the VCP test results would show little, if any, volume increase. Therefore, the

conditions of the CCP test are such that inordinate degrees of volume change are imposed on the specimen, thereby yielding results that erroneously overestimate Poisson's ratio.

CONCLUSIONS

Conclusions derived from the results of this investigation are as follows:

1. The resilient response of well-graded granular materials was independent of stress pulse duration. Therefore, any pulse duration in the range of those applied to pavement elements by wheel loads moving at speeds of about 15 to 70 mph (24 to 113 km/h) may be used in laboratory investigations.
2. The resilient response of a specimen determined after 25 to 100 stress repetitions was representative of the response after several thousand stress repetitions.
3. One specimen may be used to measure the resilient response over the entire range of stress levels. In addition, the stress sequence tests revealed that these stress levels could be applied to the specimen in any order without error.
4. The testing variable that affected the resilient response of the granular specimens most significantly was the applied state of stress. The stress-dependent nature of the resilient parameters is typified by the form of the predictive equations for E_r and ν_r (Eqs. 1 and 2).
5. Variations in the dry density of the specimen affected the resilient parameters. In general, the resilient modulus increased as density increased. Poisson's ratio showed no consistent variation with changes in density. The values of ν_r were very similar for all specimens at corresponding values of σ_1/σ_3 for the VCP test.
6. The effects of type of material on the resilient parameters were slight when compared to the effects of changes in stress. In general, crushed stone yielded slightly higher values of E_r than did gravel. The modulus of the blend material was normally between those of the other materials. Poisson's ratio varied only minimally from one material to another. The values of ν_r calculated for the gravel normally exceed those for the crushed stone.
7. Indications of anisotropic behavior were observed for both the CCP and VCP tests. Although it was not possible to measure the stiffness in both the lateral and axial directions, it appeared that each specimen was less stiff laterally.
8. As compared to the VCP test, the CCP test greatly overestimated Poisson's ratio. Most likely, some of the large lateral deformations observed were due to nonuniform stress and strain within the specimen. But, because the VCP test yielded values of ν_r in the range of 0.35 and 0.40, conditions of the CCP test could impose greater amounts of volume change on the specimens, as indicated by the computed values of ν_r consistently in excess of 0.50.
9. Values of the resilient modulus computed from CCP test data exceeded E_r values computed from the VCP tests for most stress levels. The magnitude of the difference was itself a function of stress and, thus, nonconstant.
10. Although the CCP test yielded unacceptably high values of Poisson's ratio, the use of a constant value from ν_r for granular paving materials in the range of 0.35 to 0.40 adequately represented this parameter for pavement analysis. This conclusion is based on the relatively flat slope of the regression line for ν_r over a range of σ_1/σ_3 from 2 to 7.

Before conclusions can be drawn regarding the significance of the variations in resilient parameters obtained by different test procedures (CCP or VCP), it is first necessary to examine these differences in the context of their effects on the response of a pavement structure to wheel loadings.

REFERENCES

1. Allen, J.J. The Effects of Non-Constant Lateral Pressures on the Resilient Response of Granular Materials. Univ. of Illinois at Urbana-Champaign, PhD dissertation, May 1973.
2. Barksdale, R.D. Compressive Stress Pulse Times in Flexible Pavements for Use in Dynamic Testing. Highway Research Record 345, 1971, pp. 32-44.

3. Barksdale, R. D. Repeated Load Test Evaluation of Base Course Materials. Georgia Inst. of Tech., Atlanta, Proj. E20-609, Dec. 1971.
4. Barksdale, R. D., and Hicks, R. G. Material Characterization and Layered Theory for Use in Fatigue Analyses. HRB Spec. Rept. 140, 1973, pp. 20-48.
5. Dehlen, G. L. The Effect of Non-Linear Material Response on the Behavior of Pavements Subjected to Traffic Loads. Univ. of California, Berkeley, PhD dissertation, 1969.
6. Dunlap, W. A. A Report on a Mathematical Model Describing the Deformation Characteristics of Granular Materials. Texas Transportation Institute, Texas A&M Univ., College Station, Tech. Rept. 1, Study 2-8-62-67, 1963.
7. Gray, J. E. Characteristics of Graded Base Course Aggregates Determined by Triaxial Tests. Nat. Crushed Stone Assoc., Washington, D.C., Engineering Bull. 12, July 1962.
8. Hicks, R. G. Factors Influencing the Resilient Properties of Granular Materials. Univ. of California, Berkeley, PhD dissertation, 1970.
9. Moore, W. M., Britton, S. C., and Scrivner, R. H. A Laboratory Study of the Relation of Stress to Strain for a Crushed Limestone Base Material. Texas Transportation Institute, Texas A&M Univ., College Station, Res. Rept. 99-5F, Study 2-8-65-99, Sept. 1970.
10. Morgan, J. R. The Response of Granular Materials to Repeated Loadings. Proc. Third Conference of Australian Road Research Board, Sydney, 1966, pp. 1178-1192.
11. Seed, H. B., Mitry, F. G., Monismith, C. L., and Chan, C. K. Prediction of Flexible Pavement Deflections from Laboratory Repeated-Load Tests. NCHRP Rept. 35, 1967.